

Please note! This is a self-archived version of the original article.

Huom! Tämä on rinnakkaistallenne.

To cite this Article / Käytä viittauksessa alkuperäistä lähdettä:

Badara, O., Rämö, V., Rissanen, M. & Tehrani-Bagha, A. (2024) Mechanically recycled textile fibers in carded and needle-punched non-wovens : Implications on processability, structure, and performance. *Textile Research Journal*, 2024.

URL: <https://doi.org/10.1177/00405175241302482>

# Mechanically recycled textile fibers in carded and needle-punched non-wovens: Implications on processability, structure, and performance

Textile Research Journal

0(0) 1–20

© The Author(s) 2024



Article reuse guidelines:

[sagepub.com/journals-permissions](https://sagepub.com/journals-permissions)

DOI: 10.1177/00405175241302482

[journals.sagepub.com/home/trj](https://journals.sagepub.com/home/trj)

Olamide Badara<sup>1,2,\*</sup> , Virpi Rämö<sup>1,2,\*</sup>, Marja Rissanen<sup>2</sup> and Ali Tehrani-Bagha<sup>1</sup>

## Abstract

To foster a circular economy, it is crucial to increase the recycling of solid waste significantly, particularly post-consumer textile waste, and identify viable applications for the reclaimed materials. This study specifically examined the integration of mechanically recycled post-consumer polyester and cotton fibers containing fractions into carded and needle-punched non-woven structures. The research investigated the carding processability of four mechanically recycled fibers, examining their performance when combined with virgin polyester fibers in varying ratios. The fiber fractions were characterized in terms of mean fiber length, short fiber content, fiber uniformity, diameter, fiber bundle strength, and elongation. The processability challenges encountered during the carding of the mechanically recycled textile fractions were mainly associated with high proportions of synthetic recycled fibers, which resulted in increased fiber piling on the metallic parts of the carding device. Furthermore, the effect of different blend ratios of mechanically recycled polyester and cotton fibers with virgin polyester fiber on the properties of carded and needle-punched structures, including mass per unit area, thickness, tensile strength, elongation, air permeability, morphology, and porosity was studied. The tensile properties and air permeability of non-wovens obtained from 50/50 blends of recycled polyester cotton and virgin polyester were comparable to those produced from 100% virgin polyester fibers. The results of this study demonstrate that carding and needle punching provide a robust route for processing polyester and cotton containing mechanically recycled end-of-life textile-based fractions without the use of chemical additives.

## Keywords

carding, textile waste, post-consumer textile, fiber length distribution, needle punching, non-wovens, mechanical properties

Mechanically recycled textile fibers are an increasingly available raw material source for versatile applications due to developing EU regulations. Consequently, new research on the processability and performance of this material is essential to support the development of new commercial applications. Approximately 5.8 million tons of textile waste is generated in Europe annually.<sup>1</sup> However, 87% of this waste ends up in the landfill or is incinerated.<sup>2</sup> The heterogeneous nature of textile waste as well as the presence of additives such as dyes and finishings create challenges for recycling.<sup>3</sup> EU legislation requires separate collection of textile waste by 2025, which will increase the accessibility of textile waste as a raw material source.<sup>4</sup> Furthermore, EU countries are required to progressively increase their recycling rates, targeting 55% of their municipal

waste by 2025, 60% by 2030 and 65% by 2035.<sup>5</sup> Thus, there is a need to find broader applications and develop commercial uses and markets for this fiber material to enhance the circular economy.

Several approaches have been developed to recycle post-consumer textile waste into new raw materials.

<sup>1</sup>School of Chemical Engineering, Aalto University, Espoo, Finland

<sup>2</sup>School of Built Environment and Bioeconomy, Tampere University of Applied Sciences, Tampere, Finland

\*These authors contributed equally to this work.

## Corresponding author:

Olamide Badara, Aalto University, Vuorimiehentie 1, 02150 Espoo, Finland.

Email: [olamide.badara@aalto.fi](mailto:olamide.badara@aalto.fi)

These include mechanical, chemical, and biochemical methods.<sup>6-8</sup> Mechanical recycling involves sorting and cleaning post-consumer textiles, followed by the disintegration of these textiles into individual fibers using mechanical forces.<sup>7</sup> This process typically involves feeding the textiles into rotating drums with steel spikes or pins. Although the mechanical method offers benefits such as scalability and versatility, it results in fibers with reduced physical properties.<sup>9</sup> The harsh tearing process leads to fiber length shortening, a wide distribution of fiber lengths, a high short-fiber ratio, and the presence of textile remnants, such as yarns. This often results in reclaimed fibers that are shorter, less uniform and weaker than their virgin counterparts.<sup>10,11</sup> The overall characteristics of the fibers are determined by the tearing process and the heterogeneous nature of the original fabric materials, making it difficult to clearly define the properties of the reclaimed fibers.<sup>10</sup> Furthermore, because mechanical processing does not involve color removal, the resulting fibers may have varying colors, which can limit their use in certain applications.

To tackle the problems resulting from reduced fiber strength and length due to mechanical recycling of textile materials, different strategies have been employed. One such strategy involves blending mechanically recycled fibers with virgin fibers to improve the overall strength and length distribution of the resultant fibers.<sup>6</sup> Another approach involves the introduction of pre-treatments such as polyethylene glycol (PEG). The treatment of cotton and polyester-based textiles with PEG prior to textile tearing during mechanical recycling has been demonstrated to reduce damage and preserve the length of resulting recycled fibers.<sup>11</sup>

Post-consumer textiles can also be recycled chemically using methods that break them down into their constituent monomers or various intermediates via processes such as depolymerization. Conversely, the biochemical recycling route employs enzymes to selectively disintegrate certain fiber types. This method offers the advantage of reduced environmental impact and selectivity. However, its extensive application is limited due to long processing times. While chemical and biochemical recycling methods offer the advantage of producing fibers with properties comparable to virgin fibers, these techniques often tend to be more complex, expensive, and less scalable when compared with mechanical recycling.<sup>7,8</sup> Another important benefit of mechanical recycling is that despite its limitations, it allows for high recovery rates, making it a viable choice for large-scale textile waste processing.<sup>8</sup> The versatility of mechanical processing enables the manufacture of non-wovens, which can handle a broad range of fiber lengths. This versatility makes non-woven

production an attractive option for mechanically recycled fibers utilization.<sup>7</sup>

Non-wovens are one relevant application for mechanically recycled post-consumer textile fibers. For example, mechanically processed waste fibers of natural and synthetic origin have been incorporated into carded and needle-punched structures and utilized in horticulture applications, such as capillary matting and hanging basket lining, where efficient water distribution to plant roots is essential.<sup>12</sup> Further, non-wovens have been shown to be useful in durable applications, such as acoustic and thermal insulation in automobiles, carpet underlayment, and cushions to cover spring units in mattresses and furniture.<sup>12</sup>

The carding process is a web-formation process that involves the disentangling, mixing, cleaning, distribution, and layering of fibers to form uniform webs. This is achieved with the aid of a toothed cylinder, worker, and stripper rollers. During the carding process, fibers tend to break or elongate permanently. The key parameters that determine carding performance include fiber breakage, web cohesion, and uniformity of web weight. These parameters are significantly affected by the properties of the fiber feedstock, including length distribution, elongation and tenacity, fiber-to-fiber cohesion, diameter, fiber finish, and crimp.<sup>13</sup> The mean length of fibers used in most carded non-woven applications is between 38 and 100 mm.<sup>13</sup> Typically, long natural and synthetic fibers with lengths of about 38, 48, and 51 mm are utilized in the carding process.<sup>14</sup> Shorter fibers are considered to be challenging to card since they are not easily carried along by the rollers during the carding process.<sup>14</sup> To improve processability, short or stiff fibers are usually blended with longer fibers, which serve as carrier fibers to extend the fiber length distribution.<sup>13</sup>

Needle punching is a mechanical web-consolidation process that involves the repeated stroking of an array of barbed needles through a moving fiber web. Fibers are trapped by the needle's barbs and conveyed from the web surface into the web structure.<sup>15</sup> This action leads to fiber entanglement and the formation of pegs of fibers, thereby densifying and strengthening the structure without the use of chemical binders or additives.<sup>15</sup> To ensure adequate web strength, carded webs are layered to increase the mass per unit area. Cross-lapping is also employed prior to needle punching to achieve optimum tensile properties and product performance, such as permeability. Fiber properties such as crimp, length, strength, and elongation influence the efficiency of the bonding process and the non-woven properties.<sup>15,16</sup> Needle-punched structures have a fibrous network and a flexible, felt-like structure, making them ideal for filtration and drainage applications.<sup>17</sup> Needle-punched non-wovens are commonly

used in various applications, including insulation, geotextiles, roofing, blankets, carpet underlayment, and shoe felts.<sup>15,18</sup>

Halimi et al.<sup>19</sup> demonstrated that yarns and textile garment waste from blue jean manufacturing are suitable for carded and needle-punched structures. El Wazna et al.<sup>20</sup> showed that textile waste originating wool and acrylic fractions processed into non-wovens by carding and needle punching has good insulating properties and may be useful as a building insulation material. Muthu et al.<sup>21</sup> prepared insulation materials from comber noil, silk cocoon waste, and polyester/cotton flat strip waste through carding and needle punching. Tan et al.<sup>22</sup> showed that polyester/cotton textile waste-carded and needle-punched geotextiles exhibit good ultraviolet (UV) resistance. Sharma and Goel<sup>23</sup> successfully obtained carded needle-punched non-woven structures from a blend of recycled cotton and recycled PES fibers. The highest tensile and strength properties were achieved with a 30:70 blend ratio of recycled cotton and recycled PES fibers. Neznakomova et al.<sup>24</sup> demonstrated the feasibility of using needle-punched and stitch-bonded non-wovens obtained from mixed waste fibers in oil spill clean-up applications. Thus, carding and needle punching offer a flexible pathway to utilize mechanically recycled textile waste-originating fibers of various fiber lengths and types to manufacture structures with different gram-mages. This process seems to be especially beneficial for long-life products with low visual appearance requirements.

Furthermore, Ütebay et al.<sup>25</sup> investigated the effect of cotton textile waste properties on recycled fiber quality. It was found that factors such as fabric structure, prior dye treatments, size of fabric pieces fed to the shredder, and the number of shredding passages affect the length and quality of resulting fibers significantly. Aronsson and Persson<sup>26</sup> evaluated the tearing of post-consumer T-shirts and jeans, demonstrated that fiber length is affected by the degree of wear and fabric construction.

The effect of virgin fiber characteristics such as fiber type, length, and linear density on the carding process have been established in previous studies.<sup>14,27,28</sup> However, there is a clear research gap regarding the relationship between the properties of mechanically recycled post-consumer textile-based fiber fractions and carding processability as well as the influence of these heterogeneous fractions on the final properties of non-woven products. To address this gap, this study presents new findings on mechanically recycled textile-based fiber fractions containing cotton and polyester fibers. Furthermore, this study investigates the processability of mechanically recycled textile waste as

a raw material in carded and needle-punched non-woven structures.

The first research question was as follows: “*What is the impact of mechanically recycled textile waste-based fibers and their properties on carding processability?*” To answer this question, this study aimed to determine the optimal percentage of four different experimental waste fibers that can be blended with commercial virgin polyester to produce carded webs without the use of chemical additives. The main fiber properties considered in the study were fiber type and mean fiber length, short fiber content, fiber uniformity, fiber bundle strength, and elongation. During the carding process, visual observations were observed to assess processability, and any difficulties were recorded. The experimental fiber requiring the lowest amount of virgin polyester fiber for successful carding was selected for further investigation.

The second research question was “*What is the structure and performance of the resulting non-wovens?*” To address this question, carded and needle-punched non-woven structures were produced using various proportions of the selected experimental and virgin polyester fibers. The resulting non-woven structures were characterized in terms of mass per unit area, strength properties, air permeability, morphology, and porosity.

## Materials and methods

### Fiber materials

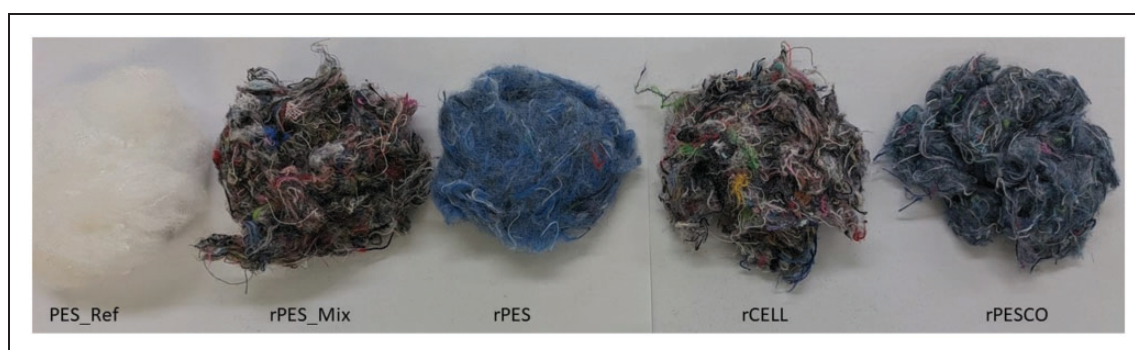
Four different mechanically recycled post-consumer textile fibers and virgin-grade polyester fibers were selected for study, as listed in Table 1. The fiber samples used in this study were selected based on commonly available recycled in recycling facilities, ensuring the practical relevance of this study. The post-consumer fibers were obtained from Finnish recycling companies Lounais-Suomen Jatehuolto Ltd., which specializes in the collection of municipal post-consumer textiles, and Rester Ltd., which focuses on post-consumer textile collection from industrial sources. Figure 1 depicts the fibers used in this study.

### Fiber opening, carding, and needle-punching procedure

The sample fibers were preconditioned at 65% relative humidity and 20°C for 24 hours before processing. In addition, all subsequent processing steps were conducted under these same conditions. The opening and blending of the fibers was performed using a Schrip type 57 fiber opener. Fibers or manually pre-blended mixtures of fibers were slowly fed into the opener, and the opened fibers were collected from the outlet.

**Table 1.** Fiber materials utilized in the experiments

Sample	Description of composition (Information given by supplier)	Origin	Source
PES_Ref	Polyester (low-grade fibers) Linear density: 1.7 dtex, Single fiber: Tenacity 28.8 cN/Text, Elongation 9.81%)	Virgin quality	Tampere University stock
rPES_Mix	Recycled polyester (70% synthetic content)	Post-consumer, mixed sources	Lounais-Suomen Jätehuolto Ltd., Finland
rPES	Recycled polyester (high polyester content)	Post-consumer, single source	Rester Ltd., Finland
rCELL	Recycled cellulose (high cellulose content)	Post-consumer, mixed sources	Lounais-Suomen Jätehuolto Ltd., Finland
rPESCO	Recycled polyester-cotton (70% polyester/ 30% cotton)	Post-consumer, single source	Rester Ltd., Finland

**Figure 1.** Photographs of the fiber materials utilized in the experiments.

Manual pre-blending was performed by weighing two different fibers in a defined ratio, spreading the first fiber on a table to form an even layer and distributing the second fibers on top as a second layer. The two fiber layers were then rolled together, and the mixed fibers were gently pulled from one end of the wrapped roll to ensure thorough blending.

The opened fiber samples were carded using a laboratory-scale carding device Automatex Model MCA 500 (line diagram illustrated in Figure 2) with a gauge speed of 10 m/min. A weighed amount of fibers was evenly distributed on the feeding table with an area of 26 cm × 50 cm. The card was turned on, and the sample was collected on a rotating sample collector wheel (doffer) as long as an even continuous web exited the card. The continuous carded web sample was cut off from the wheel to obtain a flat sheet of about 27 cm × 123 cm. Each fiber sample was carded twice to aid effective cleaning and uniformity of the webs.

Needle punching of the carded samples was performed using an Automatex Model MPR 600 needle-punching device, fitted with 15 × 18 × 40 × 3R type needles supplied by a manufacturer based in Shanghai. The samples for needle punching were prepared by layering three sheets of carded webs on top of each other. The top and bottom sheets were fed into the

needle-punching device in the machine direction, while the middle layer sheet was cut into three pieces that were twisted by 90°, thus orienting the fibers in the cross-direction. This arrangement was needle punched on one side using a punch density of 75 punches/cm<sup>2</sup>. This procedure was repeated to produce two pre-needled structures, which were combined such that the needled parts faced outwards. These combined structures were then needle punched on both sides using a punch density of 150 punches/cm<sup>2</sup>. These steps were designed and refined through preliminary trials to ensure uniformity and symmetry on both sides of the needle-punched structures. The following needle-punching parameters were utilized: ingoing belt speed 0.6 m/min and outcoming roller speed 0.5 m/min.

### Analysis of fibers

**Fiber length and strength measurements.** Fiber length and strength measurements were conducted using a Textechno FIBROTEST device, a device that is particularly suitable for mechanically recycled fibers.<sup>29</sup> The samples were prepared using a flat carding sampler. Fifteen measurements were taken for each recycled fiber sample used in this study. The mean fiber length, fiber uniformity, and short fiber index, as well

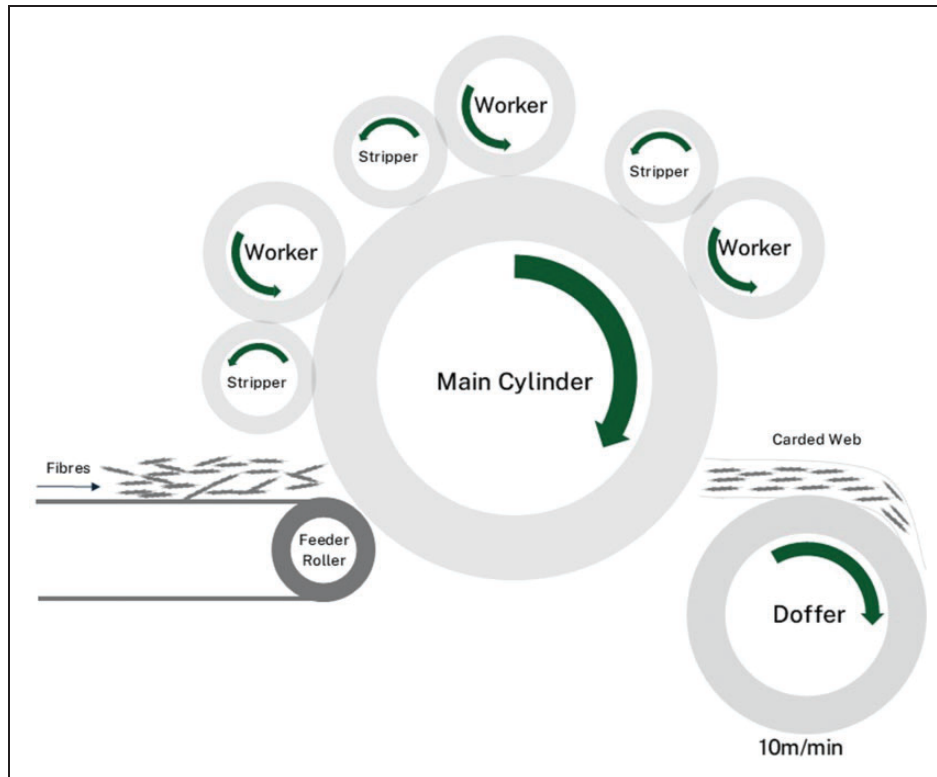


**Figure 2.** Carding machine line diagram.

as fiber bundle strength and elongation of each measurement were recorded.

**Scanning electron microscopy.** Scanning electron microscopy (SEM) images of the studied fibers were taken using a Zeiss Sigma VP electron microscope with an operating voltage of 3 kV. To ensure electric conductance, the fibers were attached to conductive carbon supports and sputtered with Au/Pt for 60 s at 20 mA. To determine the fiber diameter, SEM images were analyzed using ImageJ software. At least three images were analyzed from each sample, and 100 measurements were taken.

#### **Analysis of carded and needle-punched non-wovens**

**Mass loss during carding.** The mass loss during the carding process was determined by calculating the difference between the initial fiber mass fed into the carding device and the collected carded web. This mass loss, expressed as a percentage, was computed by dividing the mass loss by the mass of initial fiber fed into the carding device and multiplying by 100. The six carded webs produced from each fiber sample were assessed.

**Physical properties.** Mass per unit area was measured using test procedure ISO 12127:1998. Samples were preconditioned at 20°C and 65% relative humidity in

accordance with ISO 139 specifications. Five non-woven samples (100 cm<sup>2</sup>) were analyzed.

Thickness was measured using a Compac Geneve thickness gauge in accordance with the ISO 9073-2:1995 test procedure. Twenty measurements were taken from ten 100 cm<sup>2</sup> test specimens of each non-woven. The bulk density of the non-wovens was calculated by dividing the measured mass per unit area values by the measured thickness values.<sup>30</sup> Bulk density is expressed in kg/m<sup>3</sup>.

**Strength properties.** Tensile strength and elongation were assessed in accordance with standard test procedure ISO 9073-3:2023 using a tensile testing device (Testometric M350-5CT). The gauge length was 100 mm, and the rate of extension was 100 mm/min. The width of specimens was 50 mm. Five specimens of each non-woven were tested in both the machine and cross-machine directions.

Bursting strength was measured using an L&W Bursting Strength tester with a diaphragm diameter of 6.6 cm, gauge pressure of 0.26 MPa, and clamping force of 2900 N. Six 100 cm<sup>2</sup> specimens of each non-woven were assessed using standard test method ISO 13938-1:2019.

**Air permeability.** Air permeability was measured using an air permeability tester FX-3300 LabAir IV

(TexTest Instruments) according to the ISO 9073-15:2008 standard. The pressure drop utilized in this test was 100 Pa, and the surface area of samples was 20 cm<sup>2</sup>. Ten test pieces were measured for all samples except for the non-wovens containing 100% recycled content, for which seven specimens were tested due to the limited sample size. Before measurements, non-wovens were conditioned overnight in standard conditions at 65% relative humidity and 20°C according to ISO 139 specifications.

**X-ray microtomography.** A Desktom 130 tomographic scanner (Rx solutions, France) was utilized to obtain three-dimensional images of the non-wovens. The imaging parameters were as follows: acceleration voltage 40 keV, current 100 μA, rotation 360° with 1440 images, exposure time for single frame 1.25 s (no frame averaging), and total imaging time 30 mins per sample. The high-resolution three-dimensional structure and porosity data of the non-wovens were computed and obtained.

### Statistical analysis

All experimental data obtained from this study were presented as mean ± standard deviation. The normality and the equality of variances of the data were assessed using the Shapiro–Wilk and Levene’s tests, respectively.<sup>31,32</sup> For normally distributed data, the one-way analysis of variance (ANOVA) statistical method was employed to determine whether there was a statistically significant difference between the means at a 95% confidence level for fiber length, uniformity index, short fiber index, elongation, strength, and diameter data as well as for all non-woven properties evaluated in this study. The appropriate pairwise test (Tukey or Tamhane) was employed to compare group pairs and identify differences.<sup>33</sup> For non-normally distributed data, robust one-way ANOVA (Welch’s test) was utilized followed by Games–Howell test for pairwise

comparisons. All statistical tests were completed using IBM SPSS software at a 95% confidence level. The one-way ANOVA test helps to determine the likelihood of the null hypothesis, which states that there is no significant difference in the means. Conversely, the alternative hypothesis states that there is a significant difference between the means. If the probability of the null hypothesis occurring is less than 5%, the significance level is met, and the null hypothesis is rejected.<sup>33,34</sup>

## Results and discussion

### Fiber diameter, length, and strength measurements

The results for mean fiber length, short fiber index, uniformity index, bundle strength, elongation, and fiber diameter measurements are summarized in Table 2.

The mean length of the recycled fibers varied between 15.69 and 27.23 mm. PES\_Mix exhibited the highest mean fiber length value of 27.23 mm, followed by rPES which had a mean length of 21.34 mm, whereas rPESCO and rCELL had shorter fiber lengths of 15.69 and 19.51 mm, respectively. In contrast, virgin PES\_Ref fibers displayed a significantly higher mean length of 31.72 mm. Statistical analysis using one-way ANOVA and subsequent pairwise comparisons (Table 3) revealed significant differences in the mean fiber lengths of the recycled fibers, with the exception of the comparison between rCELL and rPES, which showed no significant differences.

The short-fiber index (an indication of the percentage of fibers with length less than 12.7 mm) results revealed notable differences between all the studied recycled fibers. The highest short fiber index was observed in the rPESCO fibers, whereas the lowest values was recorded for the rPES\_mix fibers.<sup>35,36</sup> In addition, all the studied textile waste-based samples exhibited higher short fiber index compared with the selected virgin PES\_Ref fibers. These observations

**Table 2.** Fiber length, diameter, strength, and elongation measurement results

	Mean length (mm)	Short fiber Index %	Uniformity Index (%)	Elongation %	Strength (g/tex)	Mean fiber diameter (μm)
rCELL	<b>19.51</b> ±2.21	<b>16.69</b> ±2.02	<b>72.21</b> ±0.99	<b>9.63</b> ±3.94	<b>8.85</b> ±2.17	<b>14.01</b> ±3.90
rPESCO	<b>15.69</b> ±0.58	<b>19.86</b> ±0.76	<b>72.93</b> ±0.77	<b>16.08</b> ±3.60	<b>10.66</b> ±3.66	<b>10.83</b> ±1.53
rPES	<b>21.34</b> ±0.80	<b>13.93</b> ±0.99	<b>74.48</b> ±0.82	<b>19.44</b> ±0.63	<b>23.40</b> ±2.06	<b>23.25</b> ±4.64
rPES_Mix	<b>27.23</b> ±2.20	<b>8.96</b> ±2.3	<b>76.49</b> ±1.59	<b>24.97</b> ±2.47	<b>15.25</b> ±2.7	<b>15.91</b> ±3.28
PES_Ref	<b>31.72</b> ±1.12	<b>0.77</b> ±0.97	<b>90.52</b> ±1.87	<b>11.95</b> ±1.07	<b>10.54</b> ±0.89	<b>14.48</b> ±2.26

**Table 3.** One-way ANOVA and pairwise test table for fiber diameter, length, strength, and elongation data of studied fibers

Groups assessed	Mean length	Short fiber index (%)	Uniformity index (%)	Elongation (%)	Strength (g/tex)	Fiber diameter
rCELL, rPESCO, rPES, rPES Mix, PES_Ref.	<0.001*	<0.001*	<0.001*	<0.001*	<0.001*	<0.001*
rCELL, rPESCO, rPES, rPES Mix.	<0.001*	<0.001*	<0.001*	<0.001*	<0.001*	<0.001*
rCELL versus rPESCO.	<0.001*	<0.001*	0.210	<0.001*	0.701	<0.001*
rPES versus rPES Mix.	<0.001*	<0.001*	0.003*	<0.001*	<0.001*	<0.001*
rCELL versus rPES.	0.054	<0.001*	<0.001*	<0.001*	<0.001*	<0.001*
rCELL versus rPES Mix.	<0.001*	<0.001*	<0.001*	<0.001*	<0.001*	0.061
rPESCO versus rPES Mix.	<0.001*	<0.001*	<0.001*	<0.001*	0.006*	<0.001*
rPESCO versus rPES.	<0.001*	0.001*	<0.001*	0.003*	<0.001*	<0.001*

$p$ -value < 0.05 indicates a significant difference: an asterisk has been added to the significant values.

$p$ -value > 0.05 indicates no significant difference.

NB: The Tamhane pairwise test for unequal variances was employed for the mean length, elongation, and strength data. Robust one-way ANOVA and Games–Howell tests were used to assess the short fiber index, uniformity index, diameter data because they failed the normality test.

were further supported by one-way ANOVA and pairwise analysis which confirmed statistical significance of the observed differences.

The uniformity index value (defined as the ratio of the average length to the average length of the longer half of fibers in a sample) for the recycled fibers ranged between 72.21% and 76.49%.<sup>35,36</sup> The lowest values were observed for rCELL (72.21%) and rPESCO (72.93%) fibers, whereas higher values were recorded for the rPES (74.48%) and rPES\_Mix values (76.49%). In addition, the virgin fibers PES\_Ref exhibited the highest uniformity index at 90.52%. Statistical analysis revealed significant differences in uniformity index between all the recycled fibers, except between rCELL and rPESCO, which showed no statistically significant difference and were therefore comparable. Higher uniformity index values indicate lower variations in fiber length distribution.<sup>37</sup>

The results of the fiber bundle strength measurements revealed differences between the recycled fibers. rPES exhibited the highest strength of 23.40 g/tex, followed by rPES\_Mix fibers at 15.25 g/tex, whereas rCELL and rPESCO exhibited significantly lower strength values of 8.85 and 10.66 g/tex, respectively. These differences were confirmed by statistical analysis, which showed a significant difference between all the recycled fibers, except for the comparison between rCELL and rPESCO fibers, where no significant difference was found. In addition, the fiber bundle elongation data indicated differences between the recycled fibers. The rPES\_Mix and rPES fibers exhibited the highest elongation properties of 24.97% and 19.44%, respectively. However, rCELL and rPESCO displayed significantly lower elongation values of 9.63% and 16.08%, respectively. These observed differences were verified by statistical analysis, which confirmed significant differences between all the recycled fibers.

The mean fiber diameter varied across the different recycled fibers. rPESCO exhibited the smallest mean diameter at 10.84  $\mu$ m, followed by rCELL at 14.01  $\mu$ m, whereas rPES\_Mix and rPES had diameters of 15.91 and 23.25  $\mu$ m, respectively, whereas the virgin PES\_Ref fibers had a mean diameter of 14.48  $\mu$ m. Among the recycle fibers, rPES fibers had the largest mean diameter, whereas rPESCO fibers had the smallest mean diameter. The observed differences between the recycled fibers were statistically significant at 95% confidence level, except for between rCELL and rPES\_Mix, where no statistically significant difference was found.

The differences observed between the recycled fibers can be associated with factors related to the inherent characteristics of the raw material fabrics, such as fiber type and blend composition. Fiber classification was based on information provided by supplier, which was used as a reference for comparative analysis. The fiber measurements results suggest that the studied recycled fibers with a higher proportion of polyester (rPES\_Mix and rPES), generally exhibited higher length, elongation, and strength, indicating higher flexibility and resilience. In contrast, the cellulose containing fibers (rCELL and rPESCO) showed reduced length, elongation, and strength, potentially reflecting increased brittleness and higher susceptibility to damage.<sup>38</sup>

In addition, the variations in fiber diameter may be linked to the measured strength properties of the recycled fibers. The rPES fibers likely maintained larger diameters due to their higher resistance to damage, as indicated by their higher strength and elongation values. In contrast, the smaller diameter values recorded of rPESCO and rCELL fibers is likely due to the presence of weaker fibers in the samples which, may have been damaged during the recycling process, as suggested by the bundle strength and elongation

results. Although rPES\_Mix demonstrated strength and elongation properties higher than those of rPESCO and rCELL, its fiber diameter may have been reduced due to the presence of other fibers that were more susceptible to damage during recycling, bringing it closer in size to the rCELL, which exhibited lower strength properties.

Beyond fiber type and composition of the recycled fibers, other unknown factors such as the level of mechanical stress and number of tearing passages applied during the recycling process, may have played a critical role in influencing the properties of the utilized recycled fibers properties.<sup>25</sup> Fibers subjected to aggressive processing may fragment further, resulting in smaller diameters, lower strength, and shorter length. In addition, other unknown factors such as variability in the original fabric structure, the original condition of the raw material fabrics such as fabric structure, extent of wear, mechanical stress, chemical treatments, or environmental exposure, during their previous lifecycle, could have introduced additional variability in the properties of the recycled fibers.<sup>19,25,26</sup> These unknown factors, while not directly related to the recycling process, likely contributed to the observed variations in the length, elongation, strength, and diameter of the studied recycled fibers. Therefore, it remains challenging to clearly explain the properties of the recycled fibers due to the complex interplay of unknown factors.

### Fiber processability in carding

A series of trial points based on Table 4 were conducted to determine whether continuous carded webs could be formed with different ratios of the sample

materials blended with virgin fibers (PES\_Ref). The fiber blends ratios used for each fiber sample were based on the Recycled Claim Standard (RCS) and Global Recycled Standard (GRS) guideline, which stipulates a minimum of 50% recycled content.<sup>39</sup> The trials began with 50% recycled content for each sample. However, in situations where achieving uniform webs was challenging at 50% recycled content, recycled content was reduced slightly to 25%.

To streamline the number of trial points, the trial plan evolved during the trial based on the visual evaluation (pass/fail) of the previous trial point. Trial points 1–11 were conducted to determine the amount of well-performing recycled fibers when blended with PES\_Ref, which is known to perform well in the used carding device. Consequently, rPESCO was selected for more comprehensive investigation at trial points 12–15, and a series of four different blend ratios together with PES\_Ref were made into carded webs. Three replicate carded webs were produced for trial points 12–15, and these replicates were then needle punched together to form a consolidated product web for further analysis.

Carding a 50/50 mixture of rPES with the reference PES\_Ref (TP1) resulted in a continuous web. However, a significant fiber loss was observed due to fibers piling to the metal knob towards the end of the trial, as shown in Figure 3. At higher tested rPES contents (75% and 100%), no continuous webs were formed. In these trials, it was observed that all fibers piled to the metal knob at TP2. In addition, the formation of a very uneven web led to a web break at TP3, as shown in Figure 4. The rPES\_Mix fibers exhibited similar behavior, and continuous webs were obtained with 25% (TP4) and 50% (TP5) mixtures with the reference

**Table 4.** Trial point list including fiber composition, processing steps, and notes for each test point

Trial point	Fiber composition					Procedure	Visual evaluation
	PES_Ref	rPES	rPES_Mix	rPESCO	rCELL		
TP1	50%	50%				Carding	Pass
TP2		100%				Carding	Fail
TP3	25%	75%				Carding	Fail
TP4	75%		25%			Carding	Pass
TP5	50%		50%			Carding	Pass
TP6	50%			50%		Carding	Pass
TP7	25%			75%		Carding	Pass
TP8				100%		Carding	Pass
TP9	50%				50%	Carding	Pass
TP10	25%				75%	Carding	Pass
TP11					100%	Carding	Fail
TP12	100%					Carding + Needle punching	
TP13	50%			50%		Carding + Needle punching	
TP14	25%			75%		Carding + Needle punching	
TP15				100%		Carding + Needle punching	



**Figure 3.** Successful carding process at TP1 (left) and the fiber piling on the metallic knob at the end of the experiment (right).

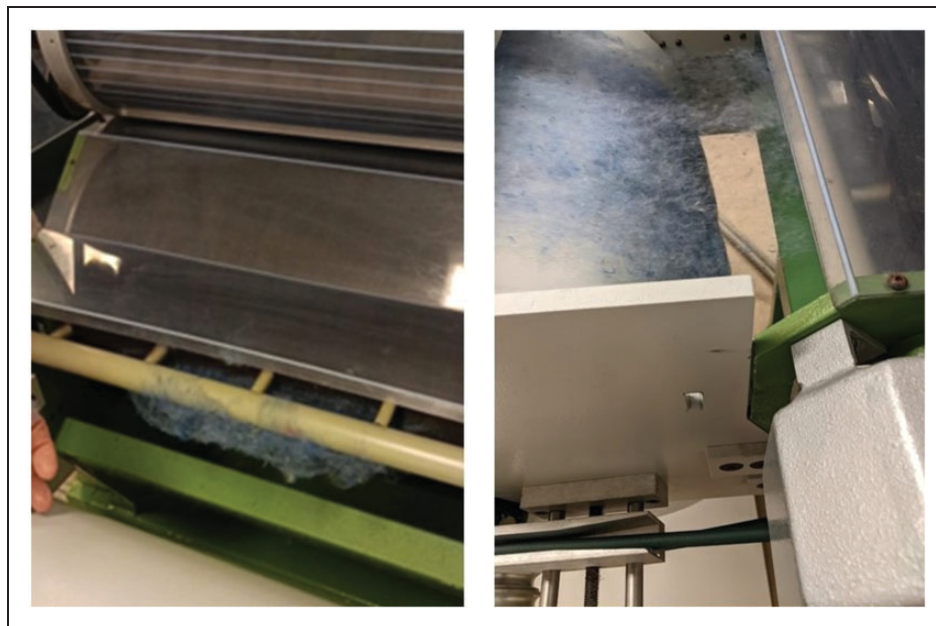


**Figure 4.** Carding process failures at TP2 (left) and TP3 (right).

fiber, whereas higher ratios of rPES\_Mix fibers were not considered relevant to test due to early indications of fiber pile-up challenges.

Although the rPES\_Mix and rPES were longer and exhibited higher elongation and strength values compared with the rCELL and rPESCO, processing difficulties encountered during carding, particularly fiber pile-up and web breakages may have originated from static electricity buildup or reduced low fiber-to-fiber

cohesion.<sup>13</sup> The persistence of this issue during carding of the rPES\_Mix and rPES fibers despite the maintenance of high humidity conditions (65% relative humidity) suggests that high polyester content played a role in the challenges encountered.

In general, the carding challenges increased considerably as the recycled fiber content increased, especially in comparison with the benchmark PES\_Ref fibers, which were processed smoothly.

rPESCO fibers were successfully carded up to 100% recycled content (TP6, TP7, and TP8). Successful carding of 100% rPESCO at TP8 is shown in Figure 5. rCELL fibers were successfully carded with 50% and 75% mixtures with the reference fibers (TP9 and TP10, respectively), justifying a further trial point with 100% rCELL. However, a continuous web was not obtained at TP11. The attraction of fibers to the metal parts of the card was reduced significantly when cellulosic fibers were present when compared with the recycled fractions with predominantly polyester content. This may be attributed to the fact that cellulosic fibers are less affected by static charges due to their higher moisture-regaining properties when compared with polyester fibers.<sup>13,40</sup> The improved carding processability of the rPESCO and rCELL fibers can also be attributed to the better fiber-to-fiber cohesion, likely due to the presence of cotton fibers. Cotton fibers are known for their twisted or natural crimp structure, which generally promotes better fiber-to-fiber cohesion during the carding process, facilitating smoother web formation.<sup>13,15,38</sup>

As expected, the reference virgin PES fibers (TP12) were carded without difficulties. The better carding processability of the virgin polyester when compared with the recycled fibers can be attributed to higher fiber length as well as the presence of fiber crimp and

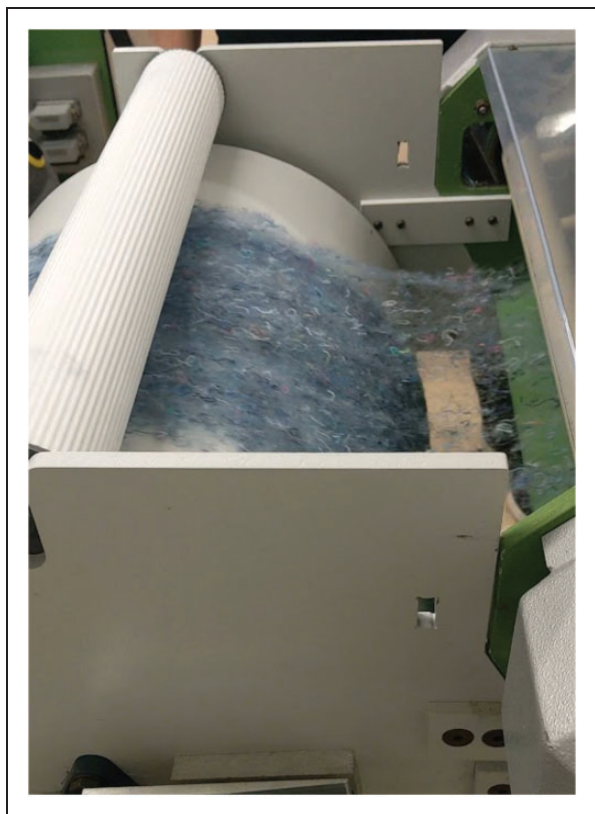


**Figure 5.** Successful carding at TP8.

possible finishes.<sup>13</sup> Commercial PES fibers often contain finishing treatments to improve their processability, as synthetic fibers are known to be prone to static electricity during the carding process.<sup>13</sup> The application of fiber finishes before carding reduces friction (fiber to fiber as well as fiber to metal), serving as lubricating agents and leading to improved fiber cohesion and less fiber breakage during the carding process.<sup>11,38</sup> Fiber finishes often contain anti-static agents to prevent the build-up of static electricity and enhance processability.<sup>11,13</sup> Static electricity can cause problems during the processing of textile fibers, as charged materials tend to attract uncharged ones, causing fibers to attach to the earthed parts of machines, which is common during the carding process.<sup>40</sup> The quantity of static electricity required to cause processing challenges varies by material and is also influenced by the level of fiber crimp.<sup>40</sup> Crimp is usually introduced to synthetic fibers to enhance frictional resistance as well as the ability of fibers to cohere under slight pressure, resulting in an overall improvement in the cohesiveness of carded webs.<sup>38</sup> Consequently, the loss of fiber crimp and finish chemicals during the laundering cycles and yarn-spinning process of post-consumer mechanically recycled textile fibers likely contributed to the lower carding processability of the recycled fibers studied in our experiments.<sup>38,40</sup>

Despite the lower uniformity index values recorded for the recycled fibers studied, the average fiber diameter likely also influenced the carding process. Finer fibers are typically expected to yield smoother, more cohesive, and uniform webs due to their high surface area per unit mass of fiber.<sup>41,42</sup> The better carding processability of the rPESCO fibers compared with the other recycled fibers may also be associated with the low mean fiber diameter recorded for rPESCO fibers, which was the lowest of all the fibers studied. The ease of carding processability of the recycled fibers tested in this study was not found to be directly related to higher mean fiber length, uniformity index, bundle strength, or elongation. This was evident in the successful carding of fiber blends containing 100% rPESCO fibers and 75% rCELL fibers, despite their shorter fiber length and lower uniformity index, bundle strength and elongation compared with rPES\_Mix and rPES.

The recycled polyester-rich fibers (rPES\_Mix and rPES) exhibited significant pile-up on the metal components of the carding device as well as web breakage issues which could not be explained by fiber length variations. Considering the differences in fiber length of the studied recycled fibers ranging between 15.7 and 27.2 mm, there was no sufficient evidence to establish a direct relationship between fiber length and carding processability. In contrast, other variables, such as

fiber type, morphology, and diameter may have had a greater influence on carding processability. Notably, the cellulose-containing (rPESCO and rCELL) recycled fibers, despite their shorter length (15.7–19.5 mm) and lower strength (8.9–10.66 g/tex), were generally easier to process than the PES-rich fibers (rPES and rPES\_Mix), which had longer lengths (21.3–27.2 mm) and higher strength (15.2–23.4 g/tex).

When comparing the strength properties of the recycled fibers and the virgin PES\_Ref fibers and correlating them with carding processability. It is worth noting that despite the relatively low bundle strength (10.54 g/tex) and moderate mean fiber length (31.72 mm) of the virgin PES\_Ref, they enhanced the carding process significantly by serving as effective carrier fibers. The longer length of the virgin PES\_Ref fibers aided fiber interlocking and improved web formation. This implies that surface features, such as friction or smoothness of the fiber, could be more important for carding performance than strength attributes alone. Despite their lower strength, the longer PES\_Ref fibers ability to aid carding emphasizes the importance of surface interactions and fiber uniformity on carding processability, particularly in fiber blends containing mechanically recycled fibers.

#### *Carded and needle-punched non-woven webs containing rPESCO fibers*

To study the influence of rPESCO fibers on the properties of non-woven structures, a series of carded webs were produced containing 0%, 50%, 75%, and 100% rPESCO together with the virgin PES\_Ref (TP12–TP15, respectively). Three carded webs were combined by needle punching into three-layered structures. This was replicated to form two pre-needled structures, which were combined, needle punched on both sides and analyzed.

*The mass loss during carding.* The mass loss during carding data (Table 5) demonstrated a clear trend of increasing fiber loss as the proportion of recycled

rPESCO fibers increased and the proportion of virgin fibers PES\_Ref fibers decreased. This indicates that the inclusion of virgin fibers improves fiber retention during carding, likely due to their longer length, which serve as carrier fibers compared with the shorter recycled fibers, which are more susceptible to being lost during the carding process.

*Physical properties.* Mass per unit area (GSM) and thickness are important parameters that influence the bulk density of non-wovens. Bulk density affects the ease of fiber movement, which plays a vital role in the mechanical properties, porosity, and permeability of non-wovens.<sup>30,43</sup> The results for mass per unit area, thickness, and bulk density are listed in Table 5.

The mass per unit area of the non-wovens produced from 0/100, 50/50, and 75/25 of rPESCO/PES\_Ref blends showed no significant statistical differences as shown in Table 6. However, a significant decrease was observed in mass per unit area of the non-wovens when the amount of rPESCO was increased to 100%, as there was significant difference between the 75/25 and 100/0 rPESCO/PES\_Ref blends. The significant reduction in mass per unit area can be explained by the fact that shorter fibers tend to have a higher ease of movement and are more prone to loss during the carding process, as they are less likely to be effectively carried by the rollers.<sup>28</sup> Therefore, when the significantly longer PES\_Ref fibers which served as carrier fibers were completely absent, this fiber loss became more pronounced, leading to a step reduction in mass per unit area. In addition, the observed increase in the weight variation was associated with the increasing loss of fibers as the recycled content increased, which is supported by mass loss measurements recorded during the carding trials.

The thickness values of the studied non-wovens ranged between 0.73 and 0.93 mm. ANOVA and Tukey pairwise analysis (Table 6) of the thickness data indicated that the thickness values of the 0/100, 50/50, and 75/25 rPESCO/PES\_Ref blends were comparable, whereas a significant difference was observed

**Table 5.** Mass per unit area, thickness, bulk density, and mass loss during carding data of the obtained non-wovens

rPESCO/PES_Ref Blends	Mass per unit area (g/m <sup>2</sup> )	Thickness (mm)	Bulk density (kg/m <sup>3</sup> )	Mass loss of during carding (%)
0/100	<b>186.02</b> ±8.15	<b>0.93</b> ±0.10	<b>202.45</b> ±22.66	<b>3.28</b> ±0.85
50/50	<b>190.40</b> ±12.73	<b>0.88</b> ±0.09	<b>217.57</b> ±23.33	<b>10.49</b> ±1.18
75/25	<b>198.74</b> ±19.35	<b>0.87</b> ±0.08	<b>230.59</b> ±21.83	<b>12.56</b> ±1.32
100/0	<b>164.36</b> ±18.45	<b>0.73</b> ±0.12	<b>231.7</b> ±41.38	<b>19.84</b> ±2.30

**Table 6.** One-way ANOVA and pairwise test table for mass per unit area, thickness, and density data of studied non-wovens

<i>p</i> -values at 95% confidence level			
Population assessed rPESCO/PES_Ref Blends	Mass per unit area	Thickness	Density
0/100, 50/50, 75/25, 100/0	0.017*	<0.001*	0.005*
0/100, 50/50, 75/25	0.384	0.103	0.001*
50/50 versus 75/25	0.826	0.960	0.379
50/50 versus 100/0	0.070	<0.001*	0.719
50/50 versus 0/100	0.968	0.482	0.239
75/25 versus 100/0	0.013*	<0.001*	1.000
75/25 versus 0/100	0.570	0.224	0.002*
0/100 versus 100/0	0.157	<0.001*	0.055

*p*-value < 0.05 indicates a significant difference: an asterisk is added to the significant values.

*p*-value > 0.05 indicates no significant difference.

NB: The Tukey pairwise test for equal variances was used for all the above forementioned data.

between 100% rPESCO sample and the other blends. This reduction in thickness can be attributed to a decrease in the fiber mass within the needle-punched non-woven structure, as reflected by the mass loss data obtained during the carding process. This reduction in fiber content results in a decrease in the overall material bulk, contributing to the observed reduction in thickness. A reduction in thickness is expected as the fiber content within the needle-punched non-woven structure decreases.<sup>44</sup>

The bulk density data analyzed using one-way ANOVA and Tukey pairwise comparisons (shown in Table 6), showed that the bulk density values of the non-wovens were generally comparable. However, the 100% PES\_Ref non-wovens exhibited significantly lower bulk density values compared with the non-wovens consisting of 75/25 blend of rPESCO and PES\_Ref. This suggests that the influence of the short, recycled fibers on the density of the non-woven structure was more evident when rPESCO fiber loading reached 75 wt%. The higher bulk density observed in the 75/25 rPESCO/PES\_ref blend can be attributed to the presence of optimal amounts of shorter recycled fibers and longer virgin PES fibers in the fiber blend. The longer virgin fibers served as carrier fibers which provided facilitated efficient fiber interlocking. This improved inter-fiber interaction improved bulk density, as the shorter recycled fiber effectively filled the voids between the longer fibers as a result of their higher short fiber content, which resulted in tighter fiber packing. In addition, higher variations in bulk density were observed for samples containing 100% rPESCO fibers.

**Tensile properties.** Figures 6 and 7 display the graphs of mean maximum tensile stress versus mean elongation

at break of the non-wovens containing 0/100, 50/50, and 75/25 rPESCO and PES\_Ref fibers, in the machine direction and cross-machine direction, respectively. The values ranged from 8.7 to 15.8 kPa in the machine direction and from 3.6 to 7.9 kPa in the cross-direction. Non-wovens prepared from 100% rPESCO fibers exhibited a significantly low tensile strength below 5 N (the sensitivity limit of the measuring device). As a result, the test equipment utilized could not recognize the maximum breaking point; hence, elongation results were also unobtainable. The maximum tensile stress of the 0/100 and 50/50 rPESCO and PES\_Ref blends were comparable in both the machine and cross-directions. In addition, a significant decrease in tensile stress was observed as the rPESCO content increased to 75% and the PES\_Ref fiber content decreased to 25%. This result is similar to results obtained by Halimi et al.<sup>19</sup> This finding was verified by the ANOVA and pairwise comparison analysis, as listed in Table 7. The computed *p*-values obtained from the pairwise comparisons of the tensile stress data of the 0/100 and 50/50 rPESCO/PES\_Ref samples were greater than 0.05, indicating that there were no significant differences between the samples. However, a pairwise comparison between 75/25 blend samples and the other samples resulted in *p*-values less than 0.05, indicating that the 75/25 blends exhibited statistically significant lower tensile stress values.

The reduction in tensile stress values may be associated with the shorter fiber length of the rPESCO fibers. This is because very short fibers tend to minimize effective web consolidation or fiber entanglement during the needle-punching process since fibers need to be long enough to be conveyed by the barbs of the needles.<sup>15</sup> The effect of shorter fibers became more evident as the rPESCO content increased from 50% to 75%. Meanwhile, non-wovens obtained from 100% PES\_Ref fibers displayed the highest tensile strength properties. This indicates that the inclusion of PES\_Ref fibers helped to improve bonding of the non-wovens consisting of 50/50 and 75/25 blends of rPESCO and PES\_Ref fibers.

The elongation at break data of the non-wovens obtained from 0/100, 50/50, and 75/25 blends of rPESCO and PES\_Ref. The values ranged from 56% to 65% in the machine direction and 123% to 132% in the cross-machine direction. The non-wovens exhibited comparable elastic properties in both the machine and cross-directions. This observation was confirmed by the ANOVA and pairwise comparison results, which are presented in Table 7. The calculated *p*-values for the elongation data of the 0/100, 50/50, and 75/25 blends of rPESCO and PES\_Ref were greater than 0.05, suggesting that there were no significant differences between the non-wovens. However, due to the

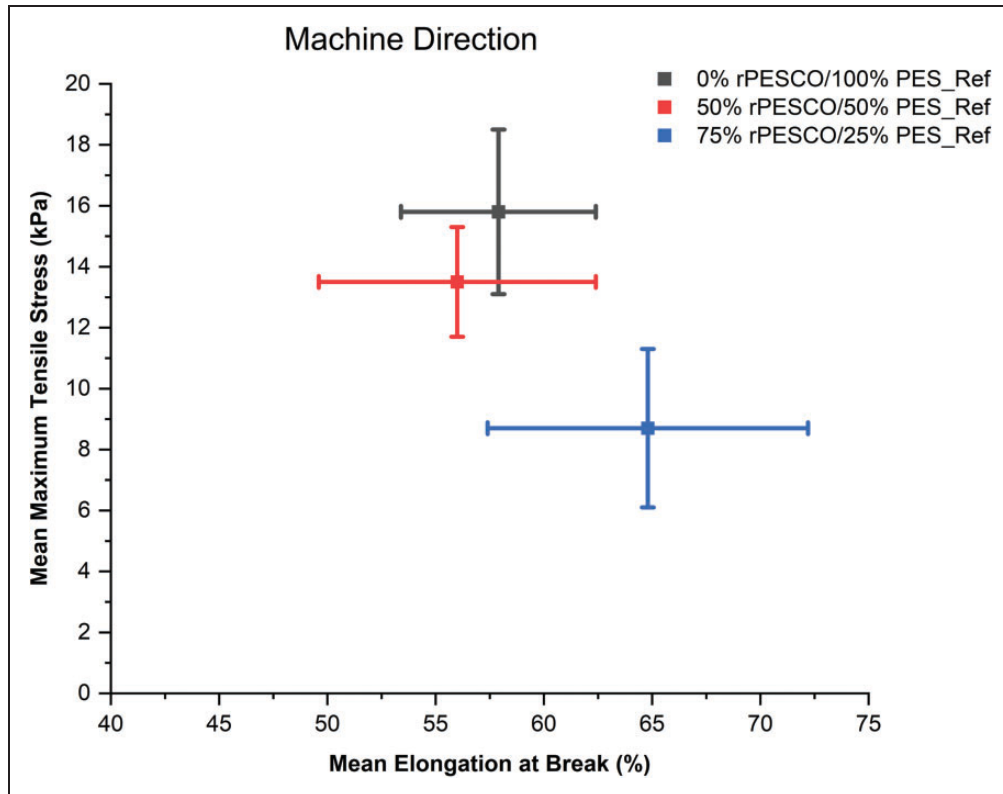


**Figure 6.** Mean maximum tensile stress versus mean elongation at break (machine direction) of the non-wovens produced from rPESCO and PES\_Ref fibers.

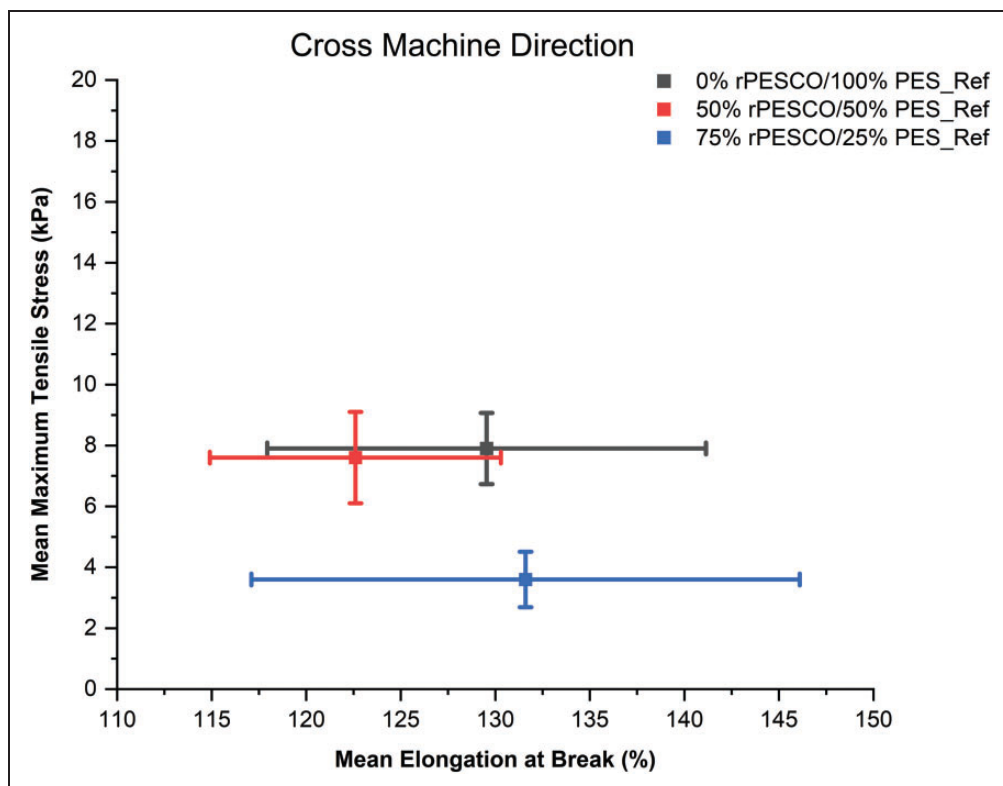


**Figure 7.** Mean maximum tensile stress versus mean elongation at break (cross-machine direction) of the non-wovens produced from rPESCO and PES\_Ref fibers.

**Table 7.** One-way ANOVA and pairwise test table for tensile stress and elongation data of studied non-wovens

<i>p</i> -values at 95% confidence level				
Population assessed rPESCO/PES_Ref blends	Tensile stress (MD)	Tensile stress (CD)	Elongation (MD)	Elongation (CD)
0/100, 50/50, 75/25	0.001*	0.001*	0.099	0.464
50/50 versus 75/25	0.018*	0.004*	0.101	0.463
50/50 versus 0/100	0.272	0.910	0.882	0.627
75/25 versus 0/100	0.001*	0.001*	0.218	0.957

*p*-value < 0.05 indicates a significant difference: an asterisk is added to the significant values.

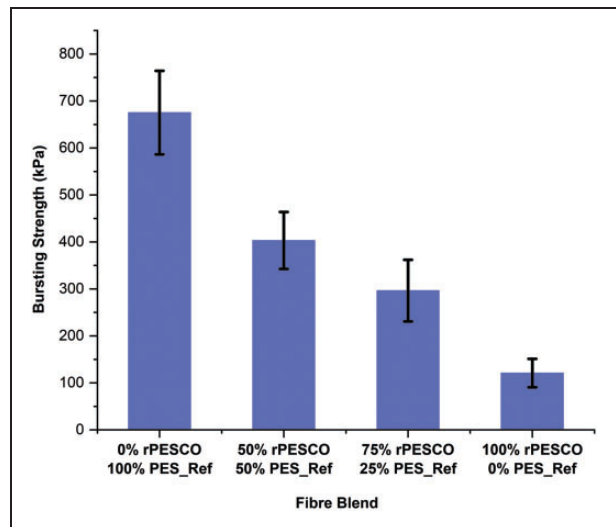
*p*-value > 0.05 indicates no significant difference.

NB: The Tukey test for equal variance was employed for the above data, whereas robust ANOVA and Games–Howell tests were employed to assess the tensile stress (CD) data because the data failed the normality test.

extremely low results, it was not possible to assess the elongation properties for the 100% rPESCO sample. This finding indicates that the elastic properties of the studied non-wovens were significantly influenced by fiber length. The comparable elongation values of the other samples containing 0/100, 50/50, and 75/25 blends of rPESCO and PES\_Ref fibers suggest that the longer PES\_Ref samples formed a coherent bonded matrix within the needle-punched structures. Conversely, rPESCO fibers were so short that they did not participate effectively in the bonded matrix and, thus, did not affect the elongation properties of the non-wovens significantly.

Based on the tensile properties results, the non-wovens produced from 0/100 and 50/50 rPESCO and PES\_Ref fiber blend based can be considered in Class 1 standards for light equipment in geotextile applications. The non-wovens exhibit the required tensile strength and elongation properties to meet the requirements for low-level service conditions as outlined in the European harmonized standards for geotextiles.<sup>45</sup>

**Bursting strength.** The bursting strength data of the non-wovens are displayed in Figure 8. The results show that bursting strength decreased as the amount of rPESCO increased, with values ranging from 52 to 606 kPa. The non-wovens obtained from 100% PES\_T fibers exhibited the highest bursting strength properties, whereas the non-wovens obtained from 100% rPESCO fibers exhibited the lowest bursting strength properties. All the non-wovens produced from the 50/50 and 75/25 blends of rPESCO and PES\_Ref fibers demonstrated lower bursting properties when compared with the 100% PES\_Ref-based non-wovens. As listed in Table 8, the ANOVA and pairwise comparison analysis confirmed a significant stepwise reduction in bursting strength as rPESCO content increased and PES\_Ref content decreased. The reduction in bursting strength of the non-wovens indicate a reduction in fiber-to-fiber interaction and frictional resistance due the reduction in longer PES\_Ref fiber content.<sup>46</sup>

**Figure 8.** Bursting strength non-wovens prepared from rPESCO and PES\_Ref fibers.**Table 8.** One-way ANOVA and pairwise test table for bursting strength and air permeability data of studied non-wovens

<i>p</i> -values at 95% confidence level		
Population assessed rPESCO/PES_Ref blends	Air permeability	Bursting strength
0/100, 50/50, 75/25, 100/0	<0.001*	<0.001*
0/100, 50/50, 75/25	0.858	0.009*
50/50 versus 75/25	0.989	0.021*
50/50 versus 100/0	<0.001*	<0.001*
50/50 versus 0/100	0.994	<0.001*
75/25 versus 100/0	<0.001*	<0.001*
75/25 versus 0/100	0.940	<0.001*
0/100 versus 100/0	<0.001*	<0.001*

*p*-value < 0.05 indicates a significant difference: an asterisk is added to the significant values.

*p*-value > 0.05 indicates no significant difference.

NB: The Tukey pairwise test for equal variances was employed for the air permeability data, whereas the bursting strength data were analyzed using the Tamhane pairwise test for unequal variances.

The bursting strength results further confirm the important role of the longer PES\_Ref fibers as carrier fibers on the structural integrity and mechanical performance of the non-woven samples produced in this study.

**Morphology of non-wovens.** Figure 9 displays SEM images of the surface of the needle-punched non-wovens produced using rPESCO and PES\_Ref fibers as recycled content (rPESCO) increased progressively from (a) to (d). Fibers can be seen across all samples, with some entanglements at specific locations across the sample. These entanglements were introduced during the needle-punching process. In addition, when comparing Figure 9(a) (100% PES\_Ref) and Figure 9(d) (100% rPESCO), a clear difference in fiber morphology can be seen. The virgin PES\_Ref fibers appear longer and have a uniform and smooth shape. In contrast, the recycled 100% rPESCO sample, consisting of a mixture of recycled cotton and polyester fibers, exhibited more irregular shapes as a result of fiber-type variations due to the presence of cotton and polyester fibers. The presence of twisted, bent fibers, as well as fibers with cracks is indicative of the presence of cotton fibers and reflect mechanical stress encountered during the tearing process.

The SEM images reveal that increasing recycled content led to a clear shift from densely packed structures, well-interlocked structures to more open structures and less interlocked fiber structures. As recycled content increased from Figure 9(b) to Figure 9(d), the fiber network became progressively more open with increased visible gaps between the fibers and reduced fiber interaction. These changes indicate that the decrease in long PES\_Ref fibers, which facilitate better inter-fiber bonding during the needling process, led to looser and more open fiber arrangements. These findings show that the introduction of short, recycled fibers rPESCO compromised tight fiber packaging and fiber interaction, resulting in a more open structure. Despite the reduction in fiber interlocking, Figure 9 (b) (50% rPESCO/50% PES\_Ref) appeared to have a balanced structure, with fewer voids, and optimal fiber interlocking.

**Tomography Images.** X-ray tomography is an effective non-destructive and non-invasive imaging method for visualizing porous structures at micro-scale in both cross-section and three dimensions.<sup>47</sup> Extensive structural information, including pore size distribution and porosity profile, can be obtained from an image

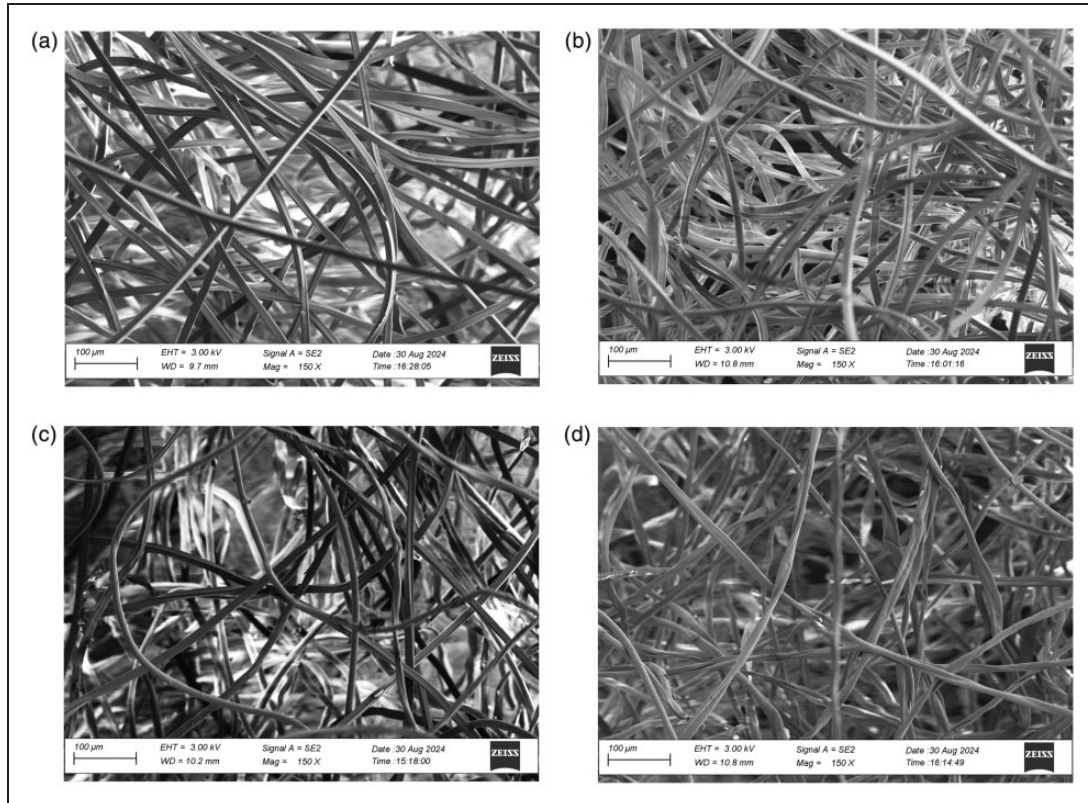


**Figure 9.** SEM images of non-wovens: (a) 0% rPESCO/100% PES\_Ref; (b) 50% rPESCO\_R/50% PES\_Ref; (c) 75% rPESCO/25% PES\_Ref and (d) 100% rPESCO/0% PES\_Ref.

analysis. Ishikawa et al.<sup>48</sup> demonstrated that X-ray tomography is a suitable tool for analyzing needle-punched non-wovens volume fraction and fiber orientation. X-ray tomography images of the carded and needle-punched structures are shown in Figure 9. The cross-section sideview images clearly show the orientation of fibers in the machine direction introduced during the carding process as well as areas of entanglement introduced by the barbed needles in the needle-punching process. Moreover, denser entangled areas are more clearly visible in samples containing the longer PES\_Ref fibers (Figure 10(a)–(c)), whereas they are less visible in the sample containing only rPESCO fibers (Figure 9(d)). This can be explained by the less-effective entanglement of the shorter fibers<sup>15</sup> and by the selected needle setup, which was designed for longer fibers and kept constant throughout the experiments.

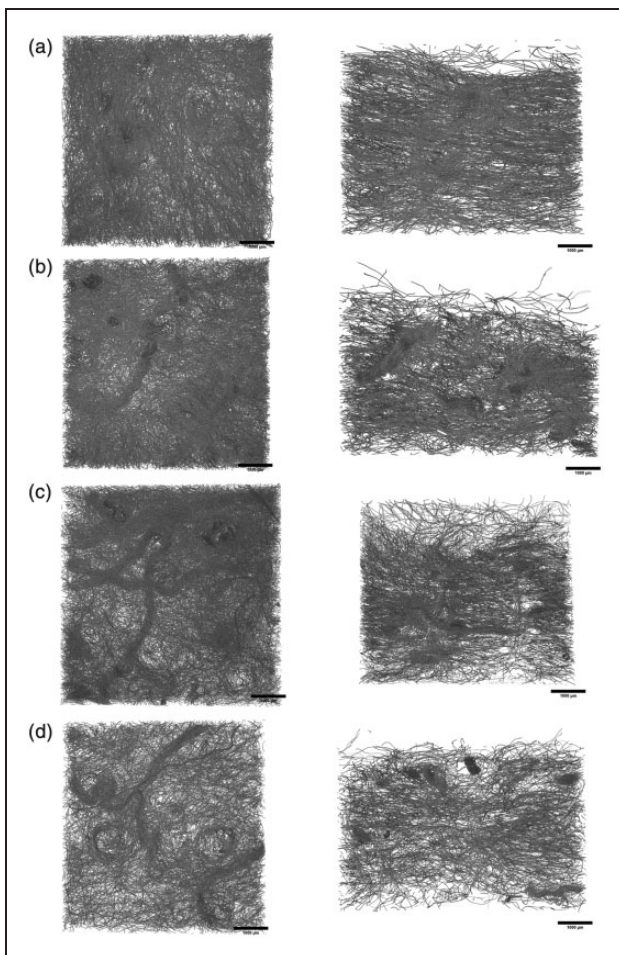


**Figure 10.** X-ray tomography structural images of a slice from above the surface (left) and a cross-section sideview (right) of carded and needle-punched structures consisting of: (a) 0% rPESCO/100% PES\_Ref fibers; (b) 50% rPESCO/50% PES\_Ref fibers; (c) 75% rPESCO/25% PES\_Ref fibers and (d) 100% rPESCO/0% PES\_Ref fibers.

This ineffective entanglement of the shorter fibers in the 100% rPESCO sample aligns with the observed reduction in strength properties. The images further highlight that as the content of the recycled fibers increased, the amount of unopened yarn and fabric pieces increased as well, which is assumed to have a further negative effect on entanglement efficiency.

When comparing the cross-sectional images obtained from X-ray tomography with those from the thickness values obtained using the thickness gauge (Table 5), it is important to note that the thickness gauge measurements reflect a compressed state due to the applied pressure during measurement. In contrast, the X-ray tomography provides measurements of the sample in an uncompressed state. Further, it should be noted that x-ray tomography represents a single spot of the sample, whereas the thickness measurement (Table 5) was performed for several parallel samples of a larger area and can, thus, be regarded as more reliable representation of the sample thickness. This discrepancy makes direct comparison between the two methods challenging, as the gauge results represent a more compacted structure. The cross-sectional images from X-ray tomography align with the thickness and GSM values reported in Table 5, particularly as the 100% rPESCO samples visually appeared to exhibit the lowest thickness and a less-compact structure when compared with the other non-woven samples.

The pore structure of non-woven materials is important, for example, in relation to liquid and gas permeability properties.<sup>49</sup> Figure 11 presents the porosity as a function of Z-position of the carded and needle-punched samples as detected by x-ray tomography imaging. The results indicated a porosity increase towards the outer surfaces of the samples, whereas porosity at the middle sections of samples appears to be more consistent and controlled. This suggests that the middle sections are more structurally stable and provide more reliable areas for comparative analysis compared to the outer sections of the samples. When comparing the Z-directional middle section (from 500 to 2500  $\mu\text{m}$  area), the 100% rPESCO sample had higher porosity when compared with all the other samples containing lower recycled fiber content. The higher porosity values at the middle part of the 100% rPESCO indicate pronounced differences in fiber interlocking during the needle punching process due to the absence of long PES\_Ref fibers.

**Air permeability.** The air permeability of non-wovens is an important parameter, for example, in dry filtration and outdoor applications, such as plant blankets, where poor ventilation can aid the growth of harmful molds and limit the proper absorption of nutrients

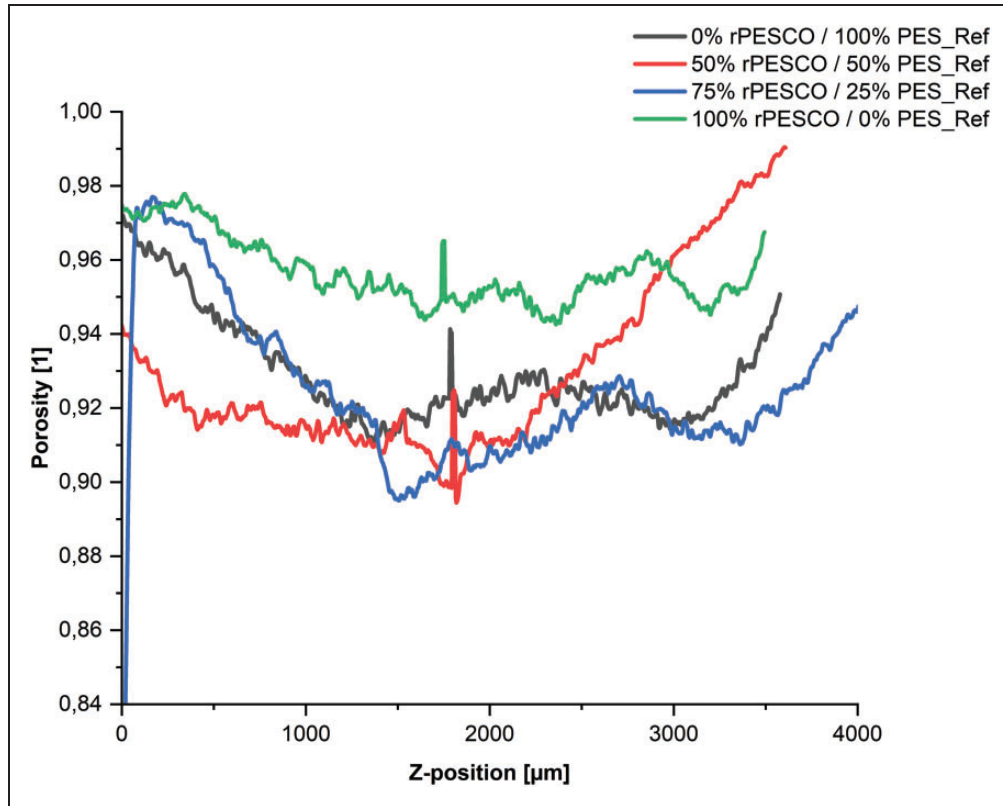


**Figure 11.** Porosity as a function of Z-position detected with X-ray tomography.

and water.<sup>22</sup> The air permeability of the needle-punched samples shown ranged from 1300 to 1700 mm/s (Figure 12). The air permeability values of the non-wovens containing 100% PES\_Ref, 50% rPESCO, and 75% rPESCO fibers were comparable, whereas a significant increase in air permeability was observed for the non-wovens prepared from 100% rPESCO fibers. This observation was supported by the ANOVA and pairwise comparison  $p$ -values (Table 8), which indicate a statistically significant difference between the 100% rPESCO-based samples and the other studied non-wovens (100% PES\_Ref, 50% rPESCO, and 75% rPESCO-containing samples).

The observations presented above could be associated with the significant reduction in the mass per unit area of the 100% rPESCO-based non-wovens. It is generally found that non-woven structures with lower weight tend to exhibit higher air permeability because of reduced resistance to air passage.<sup>28,44</sup> The higher air permeability of the 100% rPESCO sample was also consistent with the higher observed porosity of this sample. The increase in air permeability may also be associated with insufficient fiber consolidation during the needle-punching process due to the absence of long PES\_Ref fibers in the 100% rPESCO sheets.<sup>15,50</sup>

From the performance perspective, the 50/50 and 75/25 rPESCO/PES\_Ref blend samples exhibited air permeability comparable to that of the 100% PES\_Ref samples. However, both the 50/50 and 75/25 rPESCO/PES\_Ref samples demonstrated lower bursting properties compared with the 100% PES\_Ref samples. While the 100% rPESCO samples showed the highest air permeability, their tensile stress properties were too low to be measured, rendering them too fragile for practical use in applications requiring structural resilience. The 75/25 rPESCO/PES\_Ref samples also exhibited lower tensile stress properties than the 100% rPESCO samples.

The 50/50 blend provided the most balanced results, demonstrating a combination of high air permeability and tensile stress properties comparable to that of the 100% PES\_Ref samples. Furthermore, studies by Thangadurai et al.<sup>51</sup> highlight the potential of polyester-based needle punched non-wovens in industrial air filtration applications. The air permeability characteristics of the non-wovens developed in the work by Thangadurai et al. were comparable to those of the 0/100, 50/50, and 75/25 rPESCO/PES\_Ref non-wovens, indicating their potential in high air permeability applications.

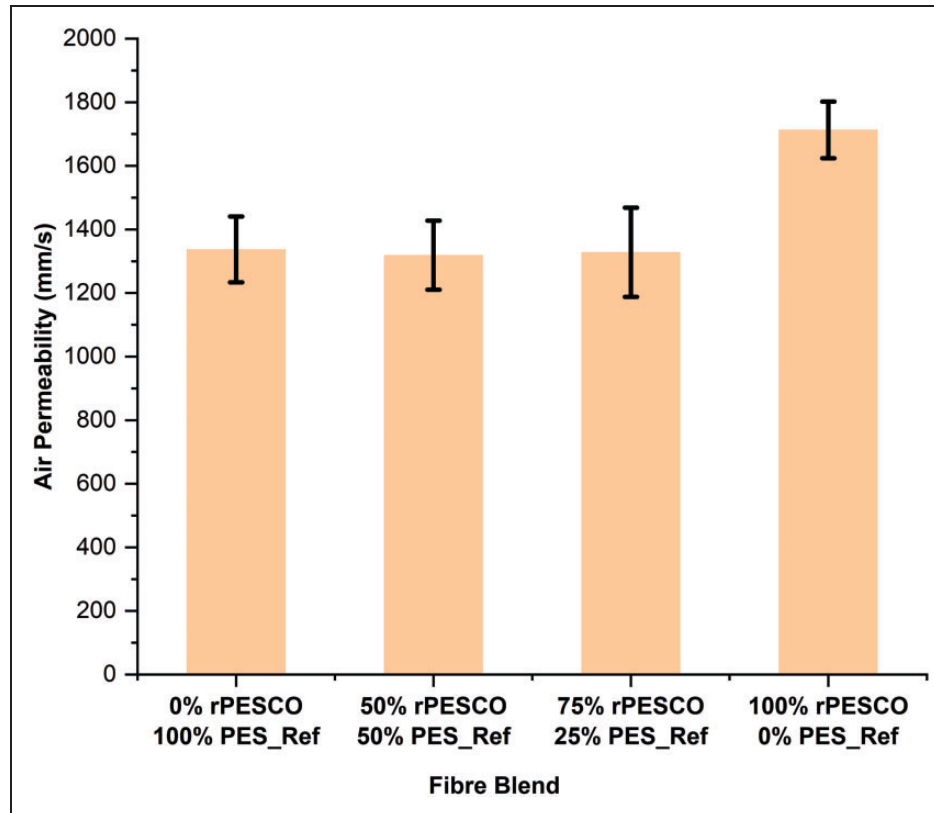


**Figure 12.** Air permeability of non-wovens prepared from rPESCO and PES\_Ref fibers.

## Conclusion

The results of this study have shown that the recycled polyester/cotton fiber fraction (rPESCO) exhibited better carding performance than the other recycled fibers investigated, allowing for successful carding with 100% recycled content. For the high cellulose content fraction (rCELL), successful carding was achieved at 75 wt% rCELL content when blended with virgin PES, while carding of the polyester-based recycled fiber samples rPES\_Mix and rPES was only successful at 50 wt% with virgin PES. The recycled polyester fractions exhibited significantly higher fiber length, strength and elongation properties than the cellulose-containing fibers, as confirmed by the ANOVA and pairwise statistical analysis. However, these properties were not seen to correlate significantly with carding processability. Thus, it was concluded that the fiber type (synthetic or containing cellulosic) had a clear effect on processability. The finding that the samples containing cellulosic fibers (rCELL and rPESCO) were easier to process than the samples containing only PES-based fibers (rPES\_Mix and rPES) was attributed to the recycled PES fibers being more prone to static electricity. The mean fiber length of the recycled samples was, in all cases, shorter than that of the reference fiber. The longer virgin polyester fibers facilitated the carding

process by serving as carriers, aiding in processing the recycled fiber fractions. The finding that the cotton containing rPESCO fibers, characterized by the smallest diameters, were the only recycled fibers successfully carded at 100 wt% without the use of processing aids suggests a future research avenue to further explore the influence of fiber diameter and fiber morphology in the recycled feedstocks.

The carded and needle-punched non-wovens containing rPESCO fibers in different ratios with virgin PES fibers highlighted the effectiveness of the longer matrix fibers in maintaining good structural and strength properties. Even when incorporating a significant share of 75 wt% of recycled rPESCO fibers, mass per unit area and thickness were well preserved while for the 100% rPESCO sample, a significant reduction in mass per unit area, thickness, tensile properties, and bursting strength was observed. Moreover, the air permeability and porosity of the non-wovens increased significantly when virgin PES fibers were absent. Bursting strength and tensile stress reduced linearly as the amount of rPESCO fibers increased, whereas air permeability and elongation remained at comparable levels in all samples containing any of the tested proportions of PES\_Ref fibers. The results indicate that longer virgin PES fibers were important as processing

aids to ensure the production of coherent carded and needle-punched structures from recycled fibers with a lower fiber length. Future research avenues are seen in investigating strategies to enhance the processability of mechanically recycled post-consumer textile fibers and enhancement of mechanical properties of the non-woven structures. Additives such as spin finish treatment to control the static electricity should be explored to further understand the role of fiber length and strength to the processability of recycled post-consumer textile fibers. Moreover, the applicability of carded and needle-punched webs containing post-consumer textile fiber fractions in composite structures could be investigated.

### Acknowledgments

The authors want to acknowledge TexTechno Germany for its contribution to the fiber length measurements, Tuomas Turpeinen (VTT) for assistance with the tomography imaging and analysis, Maija Järventausta (Tampere University) and Maria Änkö (Tampere University of Applied Sciences) for their assistance in the carding and needle-punching trials, and Tiina Ylinen (Tampere University of Applied Sciences) for assistance with the tensile strength, air permeability, and GSM measurements. Gebeyehu Esubalew Kasaw (Aalto University) provided assistance in coating the SEM samples, and Ali Tarhini and Saha Tonmoy (Aalto University) helped in the SEM imaging and analysis. Further, the authors want to acknowledge Lounais-Suomen Jätehuolto Ltd. and Rester Ltd. for providing the fiber raw materials.

### Declaration of conflicting interests

The author(s) declared no potential conflicts of interest with respect to the research, authorship, and/or publication of this article.

### Funding

This study is part of the SUSTAFIT research project (562/31/2022) funded by Business Finland 2022–2024.

### ORCID iD

Olamide Badara  <https://orcid.org/0009-0009-6247-9006>

### References

1. European Commission. *EU Strategy for Sustainable and Circular Textiles*. Brussels: European Commission, March 2022.
2. European Parliament. The impact of textile production and waste on the environment (infographics), <https://www.europarl.europa.eu/news/en/headlines/society/20201208STO93327/the-impact-of-textile-production-and-waste-on-the-environment-infographics> (2023).
3. European Environment Agency. Textile Waste, <https://www.eea.europa.eu/media/infographics/textile-waste/view> (2023, accessed 10 September 2023).
4. European Parliament. Directive (EU) 2018/851 of the European Parliament and of the Council of 30 May 2018 amending Directive 2008/98/EC on waste (Text with EEA relevance).
5. European Environmental Bureau. Waste no more: Introducing Europe's new waste laws. <https://eeb.org/waste-no-more-introducing-europes-new-waste-laws/> (2018, accessed 9 February 2024).
6. Dissanayake DGK and Weerasinghe DU. Fabric waste recycling: a systematic review of methods, applications, and challenges. *Mater Circ Econ* 2021; 3: 24.
7. Piribauer B and Bartl A. Textile recycling processes, state of the art and current developments: a mini review. *Waste Manag Res* 2019; 37: 112–119.
8. Ribul M, Lanot A, Tommencioni Pisapia C, et al. Mechanical, chemical, biological: moving towards closed-loop bio-based recycling in a circular economy of sustainable textiles. *J Clean Prod* 2021; 326: 129325.
9. Huang X, Tan Y, Huang J, et al. Industrialization of open- and closed-loop waste textile recycling towards sustainability: a review. *J Clean Prod* 2024; 436: 140676.
10. Gulich B. Development of products made of reclaimed fibres. In: *Recycling in Textiles*. Cambridge, England: Woodhead Publishing, 2006, pp. 117–136.
11. Lindström K, Sjöblom T, Persson A, et al. Improving mechanical textile recycling by lubricant pre-treatment to mitigate length loss of fibers. *Sustain Switz* 2020; 12: 1–13.
12. Gharaei R and Russell SJ. Overview of nonwoven product applications. In: *Handbook of Nonwovens*. London: Elsevier, 2022, pp. 13–47.
13. Brydon AG, Pourmohammadi A and Russell SJ. Drylaid web formation. In: *Handbook of Nonwovens*. London: Elsevier, 2022, pp. 89–179.
14. Tabor J, Wust C and Pourdeyhimi B. The role of staple fiber length on the performance of carded, hydroentangled nonwovens produced with splittable fibers. *J Eng Fibers Fabr* 2019; 14. DOI: 10.1177/1558925019832526.
15. Anand SC, Brunnschweiler D, Swarbrick G, et al. Mechanical bonding. In: *Handbook of Nonwovens*. London: Elsevier, 2022, pp. 301–393.
16. Batra S and Pourdeyhimi B. *Introduction to Nonwovens Technology*. Pennsylvania, PA: Destech Publications, 2012.
17. Ajmeri JR and Ajmeri CJ. Developments in nonwoven as geotextiles. In: *Advances in Technical Nonwovens*. Cambridge: Woodhead Publishing, 2016, pp. 339–364.
18. Shaker K, Umair M, Ashraf W, et al. Fabric Manufacturing. In: *Textile Engineering – An Introduction*. Berlin: De Gruyter, 2016, pp. 47–81.
19. Halimi MT, Hassen MB and Wannassi B. Optimization and valorization of recycled fiber in non-woven fabric. *Ind Textila* 2018; 69: 440–445.
20. El Wazna M, El Fatihi M, El Bouari A, et al. Thermo physical characterization of sustainable insulation materials made from textile waste. *J Build Eng* 2017; 12: 196–201.
21. Muthu KN, Thilagavathi G, Periasamy S, et al. Development of needle punched nonwovens from natural

- fiber waste for thermal insulation application. *J Nat Fibers* 2022; 19: 9580–9588.
22. Tan W, Fu F, Wang F-F, et al. The mechanical and ultraviolet aging properties of needle-punched nonwoven geotextiles made with recycled fibers. *J Ind Text* 2022; 51: 8668S–8689S.
  23. Sharma R and Goel A. Development of nonwoven fabric from recycled fibers. *J Text Sci Eng* 2017; 07: 1–3.
  24. Neznakovova M, Boteva S, Tzankov L, et al. Nonwoven textile materials from waste fibers for cleanup of waters polluted with petroleum and oil products. *Earth Syst Environ* 2018; 2: 413–420.
  25. Ütebay B, Çelik P and Çay A. Effects of cotton textile waste properties on recycled fibre quality. *J Clean Prod* 2019; 222: 29–35.
  26. Aronsson J and Persson A. Tearing of post-consumer cotton T-shirts and jeans of varying degree of wear. *J Eng Fibers Fabr* 2020; 15: 1558925020901322.
  27. Sengupta AK and Chattopadhyay R. Influence of fibre characteristics on hook formation during carding. *Indian J Text Res* 1988; 13: 140–142.
  28. Tabor J, Wust C and Pourdeyhimi B. The role of staple fiber length on the performance of carded, hydroentangled nonwovens produced with polypropylene fibers. *J Eng Fibers Fabr* 2019; 14: 1–14.
  29. Textechno. Recycled Fibres. *Textechno textile testing technology*. <https://www.textechno.com/applications/recycled-fibres/> (accessed 11 April 2024).
  30. Mao N. Methods for characterisation of nonwoven structure property and performance. In: *Advances in Technical Nonwovens*. Cambridge: Woodhead Publishing, 2016, pp. 155–212.
  31. SPSS tutorials. SPSS Shapiro-Wilk Test – Quick Tutorial with Example. <https://www.spss-tutorials.com/spss-shapiro-wilk-test-for-normality/> (2024, accessed 11 April 2024).
  32. SPSS Tutorials. How to Run Levene’s Test in SPSS? <https://www.spss-tutorials.com/levenes-test-in-spss/> (2024, accessed 11 April 2024).
  33. SPSS Statistics. One-Way ANOVA Post Hoc Tests. <https://www.ibm.com/docs/en/spss-statistics/29.0.0?topic=anova-one-way-post-hoc-tests> (2024, accessed 8 March 2024).
  34. Kaufman J. Analysis of variance (ANOVA). In: *Methods and Applications of Statistics in Clinical Trials*. Heidelberg: John Wiley & Sons, Inc., 2014, pp. 10–25.
  35. ASTM International. Standards Terminology Relating to Textiles. <https://www.astm.org/d0123-23.html> (2023, accessed 17 January 2024).
  36. Günaydin GK, Soydan AS and Palamutçu S. Evaluation of cotton fibre properties in compact yarn spinning processes and investigation of fibre and yarn properties. *Fibres Text East Eur* 2018; 26: 23–34.
  37. Stewart J, Oosterhuis D, Seagull R, et al. Fiber evaluation. In: *Cotton Fiber Development and Processing*. Lubbock, TX: International Textile Center, Texas Tech University, pp. 66–71.
  38. Mather RR and Wardman RH. *Chemistry of Textile Fibres*. 2nd Edition. London: Royal Society of Chemistry (RSC), 2015.
  39. Textile Exchange. The RCS and GRS are designed to boost the use of recycled materials. <https://textileexchange.org/recycled-claim-global-recycled-standard/> (2024, accessed 28 September 2024).
  40. Morton WE and Hearle JWS. Static electricity. In: *Physical Properties of Textile Fibres*. Manchester: Woodhead Publishing, pp. 665–689.
  41. Dixit P and Ishtiaque SM. Optimisation of fibre denier specific carding parameters to modulate the structure of needle-punched nonwoven. *Indian J Fibre Text Res* 2024; 49: 27–41.
  42. Seyam AM, Proffitt TJ and Velmurugan M. Role of fiber finish in the conversion of fiber to nonwovens—part II: finish performance as a mechanical processing aid in carding. *Int Nonwovens J* 2002; os-11: 30–37.
  43. Mao N, Russell SJ and Pourdeyhimi B. Characterisation, testing, and modelling of nonwoven fabrics. In: *Handbook of Nonwovens*. London: Elsevier, 2022, pp. 509–626.
  44. Çiñçik E, Koç E. An analysis on air permeability of polyester/viscose blended needle-punched nonwovens. *Text Res J* 2012; 82: 430–442.
  45. Grasso A, Farinatti E and Facchinelli V. Needle-punched nonwoven geotextile performance for separation and protection applications. <https://library.geosyntheticssociety.org/wp-content/uploads/resources/proceedings/C.17%20Needle-Punched%20Nonwoven%20Geotextile%20Performance%20for%20Separation%20and%20Protection%20Applications.pdf> (2008).
  46. Mohd Tahir AA-H, Abdul Rashid AH, Nasir SH, et al. Thermal resistance and bursting strength analysis of multilayer needle-punched bamboo/polyester nonwoven batt. *J Text Inst* 2023; 114: 974–985.
  47. Xiong Q, Baychev TG and Jivkov AP. Review of pore network modelling of porous media: Experimental characterisations, network constructions and applications to reactive transport. *J Contam Hydrol* 2016; 192: 101–117.
  48. Ishikawa T, Ishii Y, Nakasone K, et al. Structure analysis of needle-punched nonwoven fabrics by X-ray computed tomography. *Text Res J* 2019; 89: 20–31.
  49. Koponen A, Ekman A, Mattila K, et al. The effect of void structure on the permeability of fibrous networks. *Transp Porous Media* 2017; 117: 247–259.
  50. Debnath S, Chauhan VK and Singh JP. Air permeability of needle-punched filter media—virgin and recycled polyester. *J Text Inst* 2020; 111: 1159–1165.
  51. Thangadurai K, Thilagavathi G and Bhattacharyya A. Characterization of needle-punched nonwoven fabrics for industrial air filter application. *J Text Inst* 2014; 105: 1319–1326.